

# Oxidative Coupling of Coumarins by Blue-LED-Driven *in situ* Activation of Horseradish Peroxidase in a Two-Liquid-Phase System

Claudio Zippilli,<sup>\*,[a]</sup> Bruno Mattia Bizzarri,<sup>[a]</sup> Sofia Gabellone,<sup>[a]</sup> Lorenzo Botta,<sup>\*,[a]</sup> and Raffaele Saladino<sup>[a]</sup>

A blue-LED-driven two-liquid-phase system has been set up for the *in situ* activation of horseradish peroxidase avoiding the use of hydrogen peroxide and drawbacks related to enzyme denaturation and undesired radical side-reactions. The photocatalytic system was applied for the oxidative coupling of natural and synthetic coumarins to bicoumarins, allowing to obtain homodimers in only one step, avoiding the use of tedious protecting groups. Two natural C-2 symmetric bicou-

marins derived from the coupling of scopoletin were synthesized for the first time. UV-visible spectrophotometry analysis confirmed the radical-free and blue-LED-driven *in situ* oxidation of the green solvent 2-methyltetrahydrofuran to the corresponding hydroperoxide, which in turn oxidizes the ferric heme of horseradish peroxidase to ferryl intermediate, triggering the oxidative coupling reaction.

## Introduction

The activation of horseradish peroxidase (HRP) involves the heterolytic cleavage of hydrogen peroxide ( $\text{H}_2\text{O}_2$ ) with the concomitant two-electron oxidation of the heme prosthetic group to ferryl intermediate ( $\text{Fe}^{\text{IV}}$ ) and the porphyrin radical cation (Ferryl route). The  $\text{Fe}^{\text{IV}}$  active intermediate is then converted back to the resting state by sequential oxidation of two molecules of substrate.<sup>[1–3]</sup> The use of HRP in catalytic oxidation has been deeply investigated in the presence of stoichiometric amount of  $\text{H}_2\text{O}_2$ , showing critical limitations due to the inactivation of the enzyme as a consequence of undesired side-reactions.<sup>[4–9]</sup> This drawback can be avoided by slow micro-addition or by *in situ* generation of  $\text{H}_2\text{O}_2$ .<sup>[10–14]</sup> Unfortunately, slow micro-addition requires stock solutions and vigorous mixing, increasing enzyme deactivation rates, while unfavorable E-factor (mass of total waste/mass of products) and poor atom-economy were detected by *in situ* generation of  $\text{H}_2\text{O}_2$  with the traditional glucose/glucose oxidase (GOx) system.<sup>[15–17]</sup> Alternative electrochemical and photochemical procedures for the controlled generation of  $\text{H}_2\text{O}_2$  are reported, involving sacrificial electron donors.<sup>[18–25]</sup>

Another hurdle to overcome is related to the reaction medium. Indeed, HRP works in buffered aqueous media and it is usually denatured in common organic solvents.<sup>[26]</sup> Conversely, organic substrates are characterized by hydrophobic properties. The use of neat reaction conditions, or two-liquid-phase systems (2LPs), involving  $\text{H}_2\text{O}$  and a water immiscible solvent, represent a promising strategy to overcome above mentioned drawbacks, increasing reagent loading and simplifying products recovery.<sup>[27–31]</sup> The application of ethereal solvents in organic and bioorganic catalyzed oxidation has been widely described,<sup>[32,33]</sup> and 2-methyltetrahydrofuran (2-Me-THF) **1** (Figure 1) received a growing interest in recent years being a greener water-immiscible alternative to toxic THF.<sup>[34,35]</sup> In addition, compound **1** is oxidized to the corresponding hydro-

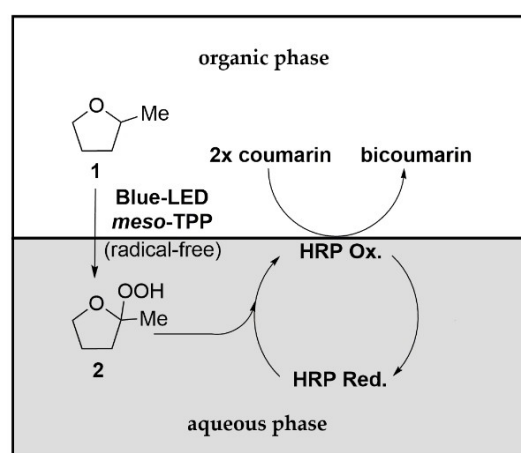


**Figure 1.** Schematic representation of blue-LED-driven 2LPs concerning the radical-free oxidation of 2-Me-THF (**1**) to hydroperoxide (**2**). This latter compound triggers the HRP-catalyzed oxidative coupling of coumarins to bicoumarins.

[a] Dr. C. Zippilli, Dr. B. M. Bizzarri, Dr. S. Gabellone, Dr. L. Botta, Prof. R. Saladino  
Department of Biological and Ecological Sciences  
University of Tuscia  
Via S.C. De Lellis s.n.c., 01100 Viterbo (Italy)  
E-mail: zippillic@unitus.it  
lorenzo.botta@unitus.it

Supporting information for this article is available on the WWW under <https://doi.org/10.1002/cctc.202100753>

© 2021 The Authors. ChemCatChem published by Wiley-VCH GmbH. This is an open access article under the terms of the Creative Commons Attribution License, which permits use, distribution and reproduction in any medium, provided the original work is properly cited.

peroxide **2** under blue-LED driven condition by direct insertion of singlet oxygen at the tertiary  $\alpha$ -etheral carbon atom (Figure 1), without formation of radical species.<sup>[36]</sup> The applications of blue-LED in photochemistry has been reported, and the role of photosensitizers, such as *meso*-tetraphenylporphyrin (*meso*-TPP) and iridium derivatives, adequately discussed.<sup>[37–39]</sup> Inspired by the ability of HRP to catalyze oxidative reactions using organic peroxides as alternative to H<sub>2</sub>O<sub>2</sub>,<sup>[40]</sup> we set up a novel blue-LED driven 2LPs for the selective coupling of coumarins to bicoumarins.

Bicoumarins are characterized by several biological properties such as anticancer, antiviral and anti-inflammatory activity.<sup>[41–43]</sup> Their synthesis usually requires multistep procedures associated to the use of tedious protecting groups, as well as hazardous reaction conditions.<sup>[44]</sup>

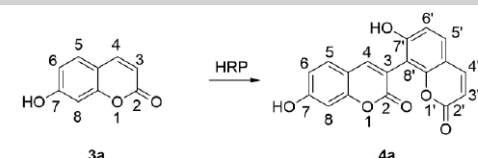
Previous synthesis of bicoumarins by a traditional HRP–H<sub>2</sub>O<sub>2</sub> approach showed poor yield and unspecific adsorption phenomena of both starting material and products on the surface of the enzyme, favored by the monophasic conditions.<sup>[45]</sup>

Here we report that bicoumarins can be efficiently synthesized in a protective group-free procedure involving the blue-LED (wavelength 470 nm) driven 2LPs, based on the radical-free *in situ* oxidation of **1** to **2** in the presence of *meso*-TPP as photosensitizer, followed by activation of HRP (Figure 1). UV-visible data confirmed the role played by blue-LED and *meso*-TPP in the formation of **2** which in turn interacts with HRP to yield the active ferryl intermediate. This procedure allowed to obtain a panel of bicoumarins in only one step avoiding unselective radical pathway, as well as the use of H<sub>2</sub>O<sub>2</sub> and radical scavengers, in higher total yields than previously reported HRP–H<sub>2</sub>O<sub>2</sub> based procedure.

## Results and Discussion

We started our investigation selecting 7-hydroxycoumarin (umbelliferon) **3a** as a model substrate. Compound **3a** (0.2 mmol) was dissolved in 2-Me-THF **1** (4.0 mL) in the presence of *meso*-TPP (1.0 mol%) followed by the addition of 2.0 mL of HRP solution (252 U/mL) in potassium phosphate buffer (PBS; 0.1 M, pH 6.0). The solution was gently stirred (200 rpm) under blue-LED irradiation (blue-LED stripes, 470 nm) and air atmosphere at 27 °C for 24 hrs. The photobioreactor was composed by a jar equipped with a liquid cooling system to stabilize the temperature at 27 ± 1 °C (for operative details see Supporting Information SI#1). After simple work-up (Materials and Methods section), 7,7'-dihydroxy-3,8'-bicoumarin **4a**, derived by the selective 3,8' oxidative C–C coupling (NMR spectra of products are in SI#2), was recovered in 80% yield, with 40% conversion of substrate **3a** (Table 1, entry 1). Compound **4a** was obtained in yields higher than previously reported for the oxidation of **3a** with traditional monophasic HRP–H<sub>2</sub>O<sub>2</sub> system, in which case a large amount of the converted substrate afforded no isolable oligomeric derivatives.<sup>[45]</sup> In accordance with the literature, the absence of C–O coupling products was probably due to adsorption phenomena of the O-centered phenolic radicals to the surface of the enzyme, affecting their

**Table 1.** Control experiments for the validation of blue-LED driven 2LPs in the HRP catalyzed coupling of **3a** to **4a**.<sup>[a]</sup>



Entry	Solvent	Light	Conversion <sup>[b]</sup> [%]	Yield <sup>[c]</sup> [%]
1 <sup>[a]</sup>	2-Me-THF	Blue-LED	40	80
2 <sup>[a,d]</sup>	2-Me-THF	Blue-LED	–	–
3 <sup>[a]</sup>	2-Me-THF	dark	–	–
4 <sup>[a,e]</sup>	2-Me-THF	Blue-LED	–	–
5 <sup>[a,f]</sup>	2-Me-THF	dark	10	42
6 <sup>[a,g]</sup>	THF	Blue-LED	2	trace
7 <sup>[a,g]</sup>	1,4-dioxane	Blue-LED	5	trace
8 <sup>[a]</sup>	AcOEt	Blue-LED	–	–
9 <sup>[a]</sup>	CH <sub>2</sub> Cl <sub>2</sub>	Blue-LED	–	–

[a] The reaction was performed starting from **3a** (0.2 mmol) and HRP (454 U) in 4.0 mL of organic solvent and 2.0 mL of PBS (0.1 M, pH 6.0), in the presence of *meso*-TPP (1.0 mol%). The reaction was gently stirred (200 rpm) under air atmosphere at 27 °C for 24 h. [b] Conversion was calculated on the basis of mmol of starting material recovered after purification. [c] Yield was calculated on the basis of mmol of converted starting material. [d] Reaction performed in absence of HRP [e] Reaction performed under argon atmosphere. [f] Reaction performed by manually adding hydroperoxide **2** prepared under Blue-LED conditions.<sup>[36]</sup> [g] Reaction performed in monophasic system. All the reactions were conducted in triplicate.

concentration in the bulk of the reaction.<sup>[45]</sup> In addition, adsorption phenomena leads to HRP denaturation, limiting substrate conversion and low mass balance of the reaction.<sup>[45]</sup> The C–C coupling occurred selectively at C-3 and C-8' position, corresponding to the energetically most stable C-centered radicals of 7-hydroxycoumarin **3a**.<sup>[46–48]</sup> To investigate the presence of oxidative side-processes related to the excitation of *meso*-TPP and the evolution of singlet oxygen, the reaction was performed under the same conditions without HRP. In this latter case no conversion of substrate was detected, highlighting that no collateral reactions, related to singlet oxygen, are involved in the blue-LED 2LPs (Table 1, entry 2). Compound **4a** was not synthesized in the absence of blue-LED irradiation or under anaerobic conditions (Table 1, entry 3 and 4 respectively), confirming the key role of blue-LED in catalyzing the formation of hydroperoxide **2**. To further confirm the ability of **2** in oxidizing HRP and triggering the oxidative homocoupling reaction, hydroperoxide **2** was synthesized (<sup>1</sup>H NMR spectrum is in SI#2),<sup>[36]</sup> and added to the reaction mixture containing HRP and **3a**, stirred under dark condition (Table 1, entry 5). The use of alternative ethereal solvents, such as tetrahydrofuran (THF) and 1,4-dioxane afforded compound **4a** in very low yield (Table 1, entries 6 and 7 respectively), as a consequence of the monophasic behavior of the system and the lower stability of 1,4-dioxane and THF hydroperoxides with respect to 2-Me-THF counterpart.<sup>[36]</sup> In addition, no conversion of **3a** was detected with non-ethereal water-immiscible organic solvents, such as ethyl acetate (AcOEt) and dichloromethane (CH<sub>2</sub>Cl<sub>2</sub>) (Table 1, entry 8 and 9 respectively).

To evaluate the stability of HRP, the enzyme was incubated under the conditions previously reported for the oxidative coupling in the absence of substrate (Table 1, entry 1). The reaction was stirred under inert atmosphere (Argon) to limit the presence of oxygen and to avoid the potential contribution of hydroperoxide **2** in the activation of HRP. At intervals, samples were taken, and the activity was evaluated spectrophotometrically by ABTS assay (Materials and Methods). The extrapolated half-life time of the enzyme was 11 h (Figure 2, green line), a value higher than that previously reported for other 2LPs.<sup>[27]</sup>

The influence of blue-LED light alone on the enzyme was also evaluated. HRP (252 U/mL) was dissolved in 2.0 mL of PBS (0.1 M, pH 6.0) and stirred under blue-LED irradiation for 24 hrs. The decreasing of activity of HRP was comparable to that of the control (dark conditions) reaching about 20% after 24 h (Figure 2, blue and black lines, respectively). This data suggests that blue-LED has no role in the deactivation of HRP and that the slow decrease of HRP activity under the blue-LED driven 2LPs was probably due to the interaction of the enzyme with **1** at the interphase layer.<sup>[27]</sup>

UV-visible spectrophotometry (Materials and Methods and SI#3) confirmed the role of **2** in the oxidation of ferric heme

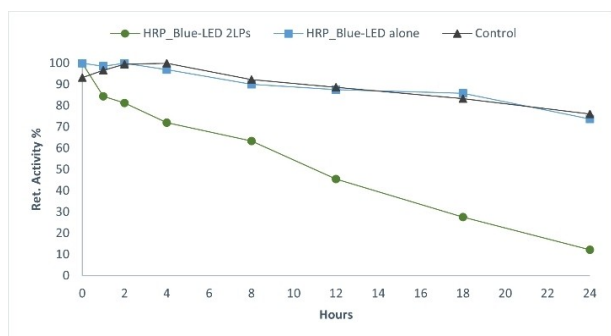


**Figure 2.** Percentage of retained activity (Ret. Activity %) of HRP at different intervals, in the blue-LED driven 2LPs (green line), under blue-LED irradiation in PBS (0.1 M, pH 6.0) in the absence of 2-Me-THF (blue line), and in dark condition as control (black line). All measurement were conducted in triplicate and expressed as average values.

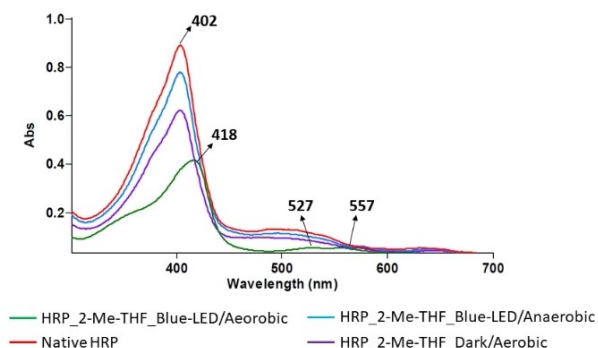


**Figure 3.** The UV-visible analysis of HRP after the addition of 2-Me-THF previously stirred under blue-LED/aerobic (green line), blue-LED/anaerobic (blue line), and dark/aerobic (violet line) conditions. The adsorption of native HRP is reported as red line.

(Fe<sup>III</sup>) to ferryl intermediate (Fe<sup>IV</sup>), a critical step for the oxidative coupling reaction. Native HRP (Fe<sup>III</sup>) is characterized by the Soret band at 402 nm and Q-band at 497 nm (Figure 3, red line). Conversely, the oxidized state (Fe<sup>IV</sup>) showed a red shift of the Soret band from 402 nm to 418 nm, and the appearance of two Q-bands at 527 nm and 557 nm, respectively.<sup>[49–52]</sup> We found that the addition of 2-Me-THF, previously stirred under blue-LED/aerobic conditions in the presence of *meso*-TPP, to a HRP buffer solution (PBS; 0.1 M, pH 6.0), effectively led to the expected red shift of the Soret band, with the concomitant appearance of the two Q-bands (Figure 3, green line). The red shift, as well as additional Q-bands, were not detected after the addition of 2-Me-THF previously stirred under blue-LED/anaerobic and dark/aerobic conditions (Figure 3; blue and violet lines, respectively). These data confirmed the relevance of **2** in the activation of HRP.

To exclude the specific presence of ·OH radicals in the blue-LED driven oxidation of **1** to hydroperoxide **2**, the reaction was repeated in the absence of HRP using coumarin **3b** as a well-recognized ·OH acceptor (“coumarin method”) (Figure 4).<sup>[53,54]</sup> In accordance with the literature, **3b** invariably reacts with ·OH at the C-7 position of the aromatic ring to yield fluorescent derivative **3a**.<sup>[55]</sup> Under our experimental conditions no traces of **3a** were detected by HPLC analysis (Materials and methods and SI#4), confirming the absence of ·OH radicals in the reaction mixture. Thus, the blue-LED driven HRP catalyzed oxidation was a useful tool in the oxidation of suitable natural substances prone to undesired side-processes in the presence of ·OH radicals.

A tentative description of the reaction pathway for the homocoupling of **3a** is described in Figure 5. In accordance with data previously reported, histidine (His) plays a key role in the formation of the ferryl intermediate by a nitrogen assisted proton transfer process.<sup>[40]</sup> In this latter case, the neighboring group participation of endocyclic oxygen of **2** in the oxidation of ferric heme (Fe<sup>III</sup>) cannot be completely ruled-out. After the delivery of the oxygen atom to HRP, hydroperoxide **2** was transformed into 5-hydroxy-pentan-2-one **5** as evaluated by GC-MS analysis (GC-MS analysis is in SI#5). Ferryl intermediate is then reduced to ferric heme by two sequential one-electron transfer steps involving HRP and two molecules of **3a** with concomitant formation of bicoumarin **4a** (Figure 5).

To generalize this procedure, the blue-LED driven 2LPs was successively applied for the oxidative coupling of a panel of

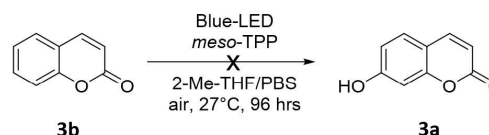


**Figure 4.** Synthesis of umbelliferon **3a** from coumarin **3b** as a specific detection method for ·OH radicals. The reaction was performed with 0.2 mmol of **3b** dissolved in 4.0 mL of 2-Me-THF and 2.0 mL of PBS (0.1 M, pH 6.0), in the presence of *meso*-TPP (1.0 mol%) under blue-LED irradiation and air atmosphere at 27 °C for 96 hrs.

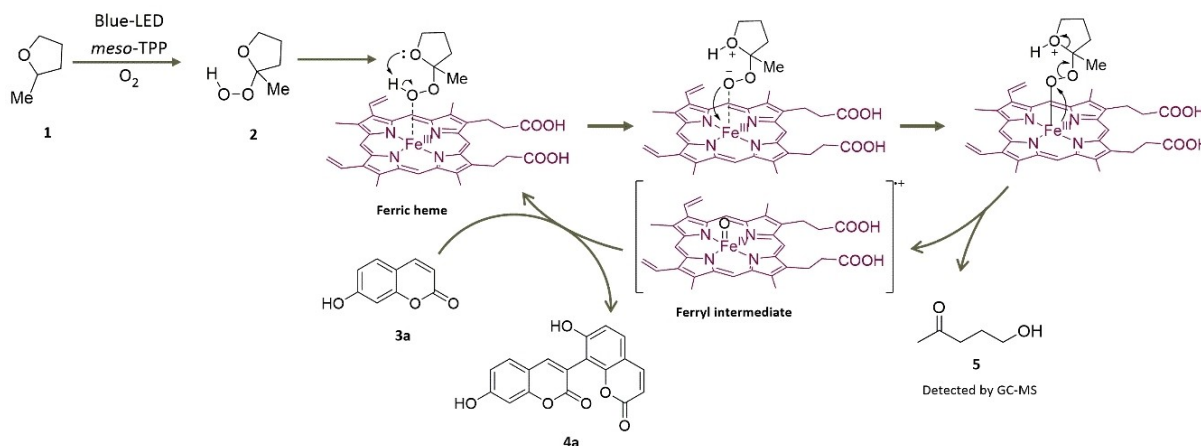


Figure 5. Proposed reaction pathway for the HRP catalyzed homocoupling of **3a** to **4a** in the blue-LED driven 2LPs.

natural and synthetic coumarins, including umbelliferon **3a**, coumarin **3b**, 7-hydroxy-6-methoxy-coumarin (scopoletin) **3c**, 4-methylumbelliferon (hymecromon) **3d**, 4-(trifluoromethyl)umbelliferon **3e**, 7-amino-4-methylcoumarin **3f** and 6-hydroxycoumarin **3g**. As described above, the reaction of **3a** with HRP in the blue-LED driven 2LPs led to 40% conversion of substrate, affording **4a** as the only recovered product in 80% yield. (Table 2, entry 1). As expected, coumarin **3b** was not converted under similar conditions being deprived of required hydroxyl group on the aromatic ring.

The absence of conversion of **3b** was a further confirmation of the absence of ·OH radicals in the photobiocatalytic system. Compound **3c**, bearing an additional methoxyl group in C-6 position, showed a different regioselectivity with respect to **3a**. In this latter case, two C-2 symmetrical bicoumarins, compounds **4c** (52%) and **4c'** (31%), were obtained as a consequence of 3-3' and 8-8' C–C coupling, respectively (numbering of compounds is reported in Table 1). At difference of **3a**, the 3-8' C–C coupling product was not recovered (Table 2, entry 3).

To the best of our knowledge, this is the first synthetic procedure for the synthesis of **4c** and **4c'** which were recently identified in *Erycibe obtusifolia* Benth (Convolvulaceae), which extracts showed strong anti-inflammatory and antiviral activity<sup>[56,57]</sup>. Compound **3d** bearing an additional methyl substituent in C-4 position showed a regioselectivity similar to **3a**, affording **4d** as the only recovered product (Table 2, entry 4).

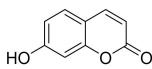
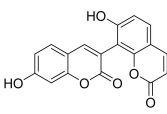
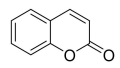
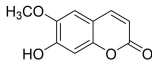
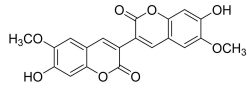
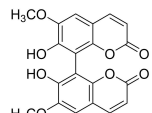
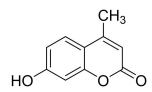
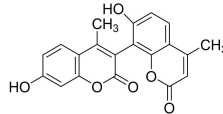
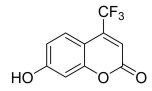
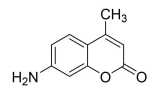
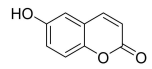
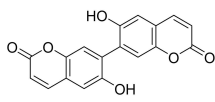
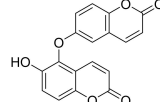
No reaction was observed in the presence of an additional trifluoromethyl substituent in C-4 position (compound **3e**; Table 2, entry 5), probably due to the high unfavorable electron withdrawing effect of the substituent.<sup>[45]</sup> The absence of reactivity was also detected in the case of 7-amino-4-methylcoumarin **3f** (Table 2, entry 6). Finally, 6-hydroxycoumarin **3g** afforded 7-7' C–C (compound **4g**) and C–O coupling (compound **4g'**) products, respectively (Table 2, entry 7). The formation of **4g'** was in accordance with the regioselectivity previously reported for the oxidation performed with HRP–H<sub>2</sub>O<sub>2</sub>

in monophasic condition<sup>[45]</sup>. Again, the blue-LED driven 2LPs led **4g'** in yields higher than previously obtained with the traditional HRP–H<sub>2</sub>O<sub>2</sub> procedure. In this latter case, the absence of reactivity in the 3-position of the pyran-2-one ring was a consequence of the lack of mesomeric stabilization forms when the OH moiety is localized in the 6-position of the aromatic ring.

## Conclusion

In conclusion, we developed a novel photobiocatalytic 2LPs involving the radical-free and blue-LED driven oxidation of 2-Me-THF **1** to hydroperoxide **2** for the activation of the heme prosthetic group of HRP, from ferric to ferryl intermediate. The activation of HRP by **2** was confirmed using UV-visible spectrophotometry analysis. The ferryl intermediate of HRP was then used as a catalyst in the regioselective coupling of hydroxyl substituted coumarins to corresponding bicoumarins. The nature of the substituent in the aromatic and pyran-2-one rings deeply influenced the regioselectivity of the coupling. As a general trend, we observed a selective coupling at C-3 and C-8 positions of the pyran-2-one and aromatic rings, respectively, in the presence of the OH moiety at C-7 position. This selectivity was lost moving the OH moiety from the C-7 to C-6 position, probably due to the absence of mesomeric stabilizing forms. Note that the prevalence of bicoumarins derived from the coupling of C-centered radicals with respect to the O-centered counterparts, may be due to the reported selective adsorption phenomena and lower stability of the latter species. This procedure led to the one-pot synthesis of bicoumarins, avoiding the use of tedious protecting group and the occurrence of undesired radical side-reactions. The unprecedented synthesis of natural bicoumarins **4c** and **4c'** from *Erycibe obtusifolia* Benth (Convolvulaceae) was also reported. Bicoumarins were obtained in high yield despite of uncomplete conversion of substrates probably due to the slow inactivation of the enzyme caused by interaction with the organic layer and adsorption phenomena.

**Table 2.** Substrate scope of HRP catalyzed homocoupling of coumarins to bicoumarins in the blue-LED driven 2LPs<sup>[a]</sup>

Entry <sup>[a]</sup>	Cpd	Structure	Conversion <sup>[b]</sup>	Product(s) (yield [%]) <sup>[c]</sup>	
1	3a		40	 4a (80)	
2	3b		No	–	
3	3c		38	 4c (52)	 4c' (31)
4	3d		45	 4d (75)	
5	3e		No	–	
6	3f		No	–	
7	3g		49	 4g (37)	 4g' (40)

[a] General experimental conditions: substrate (0.2 mmol), *meso*-TPP (1.0 mol%) and HRP (454 U) were dissolved in 4.0 mL of 2-Me-THF and 2.0 mL of PBS (0.1 M, pH 6.0). The reaction was gently stirred (200 rpm) under blue-LED irradiation and air atmosphere at 27 °C for 24 hrs. [b] The conversion of substrate was calculated on the basis of mmol of starting material recovered after purification. [c] Yield was calculated on the basis of mmol of converted starting material. All reactions were conducted in triplicate.

In this context, further studies are ongoing with the aim to improve the efficacy of the blue-LED 2LPs by using specific HRP stabilization procedure.<sup>[58,59]</sup> It is noteworthy that, the blue-LED driven 2LPs allows the activation of HRP by the radical-free and *in situ* generation of hydroperoxides **2** from the bio-renewable and ecofriendly organic solvent 2-Me-THF **1**, opening up the entry for the selective HRP functionalization of hydrophobic substrates, as well as the scaling up at industrially relevant concentration. In addition, the application of this photobiocatalytic system to chloroperoxidase and peroxygenase, are moving forward.

## Experimental Section

### Materials

Horseshoe peroxidase (EC 1.11.1.7), reagents and solvents were obtained from commercial supplier Merck KGaA, Darmstadt, Germany. UV-visible (UV-vis) spectra were recorded using Cary 60 UV-Vis spectrophotometer, Agilent, Santa Clara, USA. Chemical Reactions were monitored using thin layer chromatography on precoated aluminium silica gel Merck 60 F254 plates and a UV lamp

( $\lambda_{\text{max}}=254$  nm) was used for visualization. Merck silica gel 60 (230–400 mesh) was used for flash chromatography applying the indicated mobile phase. All products were dried in high vacuum (10–3 mbar). <sup>1</sup>H NMR and <sup>13</sup>C NMR were recorded on a Bruker Avance DRX400 (400 MHz/100 MHz) spectrometer. Chemical shifts for protons and carbons are reported in parts per million ( $\delta$  scale) and internally referenced to DMSO-*d*<sub>6</sub> signal at  $\delta$  2.50 and  $39.5 \pm 0.5$  ppm respectively. Coupling constants (*J*) are reported in Hz. Multiplicities are reported in the conventional form: s=singlet, d=doublet, t=triplet, td=triplet of doublets, q=quartet, m=multiplet, br s=broad singlet. Mass spectra (MS) data were obtained using an Agilent 1100 MSD VL system (G1946 C) interfaced with an ESI source (spray voltage of 4.5 kV and nitrogen as sheath gas). Mass spectra were acquired in positive mode scanning over the mass range from 100 to 1500 *m/z*, using a voltage of 70 mV. High-Resolution Mass Spectra (HRMS) were recorded on a LC-MS/MS system (Q Executive Plus; Thermo Scientific, MA, USA). HPLC analysis were performed by Ultimate 3000 Rapid Resolution UHPLC system (ThermoFisher scientific) equipped with Alltima C18 (250 mm × 4.6 mm, 5 mm) column and a multi wavelength detector. Blue-LED apparatus consisted in a 1.0 m blue-LED strip (wavelength 470 nm, nominal capacity/ m 14.4 W) 'LEDXON MODULAR 9009083 LED.



### HRP activity assay

The enzymatic activity of HRP was determined spectrophotometrically by 2,2'-Azino-bis(3-ethylbenzothiazoline-6-sulfonic acid) diammonium salt (ABTS) assay.<sup>[60]</sup> The assay mixture contained ABTS (1.6 mM), phosphate buffer (0.1 M, pH 6), H<sub>2</sub>O<sub>2</sub> (0.8 mM) and a suitable amount of enzyme. The oxidation of ABTS was followed by an absorbance increase at 405 nm ( $\epsilon_{405} = 36,000 \text{ M}^{-1} \text{ cm}^{-1}$ ). One unit activity of HRP is the amount of enzyme that transforms 1.0  $\mu\text{mol}$  of ABTS per minute at pH 6 at 25 °C.

### UV-visible spectrophotometric analyses of the retained activity % of HRP

The percentage of retained activity of HRP at different intervals (0, 1, 2, 4, 8, 12, 18 and 24 h) was evaluated spectrophotometrically by the ABTS assay. All analysis were conducted in triplicate and reported as average values. For the retained activity % of HRP in the blue-LED driven 2LPs, 2.0 mL of HRP solution (252 U/mL) in PBS (0.1 M, pH 6.0) was added to 2-Me-THF (4.0 mL) containing *meso*-TPP (0.002 mmol, 1.2 mg) and the mixture was gently stirred (200 rpm) under blue-LED irradiation and air atmosphere at 27 °C, for 24 hrs. At indicated intervals, samples of the buffered solution containing HRP were withdrawn and analyzed. For the retained activity % of HRP, in blue-LED alone condition, 2.0 mL of HRP solution (252 U/mL) in PBS (0.1 M, pH 6.0) was gently stirred (200 rpm) under blue-LED irradiation and air atmosphere at 27 °C, for 24 hrs. At indicated intervals, samples were withdrawn and analyzed. For the retained activity % of control HRP, 2.0 mL of HRP solution (252 U/mL) in PBS (0.1 M, pH 6.0) was gently stirred (200 rpm) under air atmosphere at 27 °C, for 24 h, and the flask was covered by aluminium foil. At indicated intervals samples were withdrawn and analyzed.

### UV-visible spectrophotometric analyses of the oxidation of the HRP ferric heme to the ferryl intermediate by 2

UV-visible spectrophotometric analyses were performed in the scan range of 250–700 nm. For the UV-visible spectrum of HRP treated with 2-Me-THF under blue-LED/aerobic condition, a solution of 2-Me-THF (2.0 mL) containing *meso*-TPP (0.002 mmol, 1.2 mg), was previously stirred for 5 min under blue-LED irradiation and air atmosphere at 27 °C. After this time 50  $\mu\text{L}$  of this solution was added to HRP in PBS (0.1 M, pH 6.0), and the analysis was recorded immediately. For the UV-visible spectrum of HRP and 2-Me-THF under blue-LED/anaerobic condition, a solution of 2-Me-THF (2.0 mL) containing *meso*-TPP (0.002 mmol, 1.2 mg), was previously stirred for 5 min under blue-LED irradiation and argon atmosphere, at 27 °C. After this time 50  $\mu\text{L}$  of this solution was added to HRP in PBS (0.1 M, pH 6.0), and the analysis was recorded immediately. For the UV-visible spectrum of HRP and 2-Me-THF under dark/aerobic condition, a solution of 2-Me-THF (2.0 mL) containing *meso*-TPP (0.002 mmol, 1.2 mg), was previously stirred for 5 min in a flask covered with aluminium foil, under air atmosphere at 27 °C. After this time 50  $\mu\text{L}$  of this solution was added to HRP in PBS (0.1 M, pH 6.0), and the analysis was recorded immediately.

### Coumarin methods for specific detection of $\cdot\text{OH}$ radicals

Coumarin **3b** (0.2 mmol) and *meso*-TPP (1.0 mol%) were dissolved in 2-Me-THF (4.0 mL), then 2.0 mL of PBS (0.1 M, pH 6.0) has been added and the mixture was stirred under blue-LED irradiation, air atmosphere, at 27 °C, for 96 hrs. The organic phase was then separated by the aqueous one, washed with brine (3  $\times$  4 mL), dried over sodium sulfate, and evaporated under vacuum. The crude

sample, standard references **3b** and **3a**, were analyzed by HPLC following the absorbance at 254 nm, using the following conditions: column temperature 30 °C, flow rate 1.0 mL/min, isocratic mobile phase composed by 60% of A (H<sub>2</sub>O) and 40% of B (MeOH), run time 30 minutes.

### General procedure for the synthesis and characterization of bicoumarins **4a**, **4c-c'**, **4d-d'** and **4g-g'**

Coumarin **3a-g** (0.2 mmol) and *meso*-TPP (1 mol%) were dissolved in 2-Me-THF (4.0 mL), then 2.0 mL of a PBS solution of HRP (252 U/mL) was added and the mixture was gently stirred (200 rpm) under blue-LED irradiation and air atmosphere at 27 °C, for 24 hrs. The organic phase was then separated by the aqueous one, washed with brine (3  $\times$  4 mL), dried over sodium sulfate and evaporated under vacuum. The crude product was purified by flash column chromatography.

**Bicoumarin 4a:**  $R_f = 0.18$  (CH<sub>2</sub>Cl<sub>2</sub>/MeOH 25:1); yellow amorphous powder (80%). <sup>1</sup>H NMR (400 MHz, [D<sub>6</sub>]DMSO):  $\delta = 8.00$  (s, 1H, CH=C=O), 7.94 (d,  $J_{\text{H,H}} = 9.6$  Hz, 1H, CH=CH-C=O), 7.60 (d,  $J_{\text{H,H}} = 8.4$  Hz, 1H, Ar-H), 7.58 (d,  $J_{\text{H,H}} = 8.4$  Hz, 1H, Ar-H), 6.83–6.71 (m, 3H, Ar-H), 6.20 (d,  $J_{\text{H,H}} = 8.4$  Hz, 1H, CH=CH-C=O) ppm. <sup>13</sup>C NMR (100 MHz, [D<sub>6</sub>]DMSO):  $\delta$ : 161.5 (Ar), 160.2 (C=O), 159.3 (Ar), 159.2 (C=O), 155.2 (Ar), 153.2 (Ar), 144.8 (CH=CH-C=O), 144.7 (CH=C=O), 129.7 (Ar), 129.2 (Ar), 114.7 (CH=CH-C=O), 113.3 (Ar), 112.5 (Ar), 111.6 (Ar), 111.1 (CH=C=O), 111.0 (Ar), 110.2 (Ar), 102.0 (Ar) ppm. MS (ESI):  $m/z$  calcd for C<sub>18</sub>H<sub>11</sub>O<sub>6</sub> = 323.05 [M+H]<sup>+</sup>; found: 323.09; HRMS (ESI):  $m/z$  calcd for C<sub>18</sub>H<sub>9</sub>O<sub>6</sub> = 321.0405 [M-H]<sup>-</sup>; found: 321.0407; elemental analysis calcd (%) for C<sub>18</sub>H<sub>10</sub>O<sub>6</sub>: C 67.09, H 3.13, O 29.79; found: C 67.06, H 3.17, O 29.84. (for the full characterization of compound **4a** see ref. [45]).

**Bicoumarin 4c:**  $R_f = 0.22$  (CH<sub>2</sub>Cl<sub>2</sub>/MeOH 30:1); yellow amorphous powder (52%). <sup>1</sup>H NMR (400 MHz, [D<sub>6</sub>]DMSO):  $\delta = 8.29$  (s, 2H, CH=CH-C=O), 7.28 (s, 2H, Ar-H), 6.82 (s, 2H, Ar-H), 3.83 (s, 6H, -OCH<sub>3</sub>) ppm. <sup>13</sup>C NMR (100 MHz, [D<sub>6</sub>]DMSO):  $\delta = 159.6$  (C=O), 151.0 (Ar), 148.9 (Ar), 145.5 (Ar), 142.8 (CH=C=O), 116.8 (CH=C=O), 110.4 (Ar), 109.6 (Ar), 102.3 (Ar), 55.9 (-OCH<sub>3</sub>) ppm. MS (ESI):  $m/z$  calcd for C<sub>20</sub>H<sub>15</sub>O<sub>8</sub> = 383.07 [M+H]<sup>+</sup>; found: 383.03; HRMS (ESI):  $m/z$  calcd for C<sub>20</sub>H<sub>13</sub>O<sub>8</sub> = 381.0616 [M-H]<sup>-</sup>; found: 381.0615; elemental analysis calcd (%) for C<sub>20</sub>H<sub>14</sub>O<sub>8</sub>: C 62.83, H 3.69, O 33.48; found: C 62.81, H 3.72, O 33.47 (for the full characterization of compound **4c** see ref. [56]).

**Bicoumarin 4c':**  $R_f = 0.19$  (CH<sub>2</sub>Cl<sub>2</sub>/MeOH 30:1); yellow amorphous powder (31%). <sup>1</sup>H NMR (400 MHz, [D<sub>6</sub>]DMSO):  $\delta = 7.99$ –7.96 (dd,  $J_{\text{H,H}} = 9.2$ , 2.0 Hz, 2H, CH=CH-C=O), 7.33 (d,  $J_{\text{H,H}} = 4.4$  Hz, 2H, Ar-H), 6.20 (d,  $J_{\text{H,H}} = 9.2$  Hz, 2H, CH=CH-C=O), 3.90 (s, 6H, -OCH<sub>3</sub>) ppm. <sup>13</sup>C NMR (100 MHz, [D<sub>6</sub>]DMSO):  $\delta = 160.5$  (C=O), 151.5 (Ar), 148.9 (Ar), 145.4 (Ar), 144.8 (CH=CH-C=O), 111.5 (CH=CH-C=O), 110.4 (Ar), 109.6 (Ar), 108.5 (Ar), 55.9 (-OCH<sub>3</sub>) ppm. MS (ESI):  $m/z$  calcd for C<sub>20</sub>H<sub>15</sub>O<sub>8</sub> = 383.07 [M+H]<sup>+</sup>; found: 383.09; HRMS (ESI):  $m/z$  calcd for C<sub>20</sub>H<sub>13</sub>O<sub>8</sub> = 381.0616 [M-H]<sup>-</sup>; found: 381.0617; elemental analysis calcd (%) for C<sub>20</sub>H<sub>14</sub>O<sub>8</sub>: C 62.83, H 3.69, O 33.48; found: C 62.84, H 3.70, O 33.46. (for the full characterization of compound **4c'** see ref. [56]).

**Bicoumarin 4d:**  $R_f = 0.19$  (CH<sub>2</sub>Cl<sub>2</sub>/MeOH 30:1); yellow amorphous powder (75%). <sup>1</sup>H NMR (400 MHz, [D<sub>6</sub>]DMSO):  $\delta = 7.71$  (d,  $J_{\text{H,H}} = 8.8$  Hz, 1H, Ar-H), 7.68 (d,  $J_{\text{H,H}} = 8.8$  Hz, 1H, Ar-H), 6.97 (d,  $J_{\text{H,H}} = 8.8$  Hz, 1H, Ar-H), 6.87–6.84 (dd,  $J_{\text{H,H}} = 8.4$ , 2.4 Hz, 1H, Ar-H), 6.78 (d,  $J_{\text{H,H}} = 2.4$  Hz, 1H, Ar-H), 6.14 (s, 1H, C=CH-C=O), 2.41 (s, 3H, CH<sub>3</sub>), 2.12 (s, 3H, CH<sub>3</sub>) ppm. <sup>13</sup>C NMR (100 MHz, [D<sub>6</sub>]DMSO):  $\delta = 161.2$  (C=O), 160.0 (Ar), 159.1 (C=O), 158.9 (Ar), 154.2 (C=CH-C=O), 153.8 (Ar), 152.6 (Ar), 151.0 (C=C-C=O), 127.0 (Ar), 126.1 (Ar), 113.9 (Ar), 113.1 (Ar), 112.5 (Ar), 112.1 (Ar), 112.0 (C=C-C=O), 110.1 (Ar), 109.5

(C=CH=C=O), 102.0 (Ar), 18.2 (CH<sub>3</sub>), 16.0 (CH<sub>3</sub>) ppm. MS (ESI): *m/z* calcd for C<sub>20</sub>H<sub>15</sub>O<sub>6</sub> = 351.08 [M+H]<sup>+</sup>; found: 351.11; HRMS (ESI): *m/z* calcd for C<sub>20</sub>H<sub>13</sub>O<sub>6</sub> = 349.0718 [M-H]<sup>-</sup>; found: 349.0716; elemental analysis calcd (%) for C<sub>20</sub>H<sub>14</sub>O<sub>6</sub>: C 68.57, H 4.03, O 27.40; found: C 68.56, H 4.04, O 27.41 (for the full characterization of compound **4d** see ref. [45]).

Bicoumarin **4g**: *R*<sub>f</sub> = 0.20 (CH<sub>2</sub>Cl<sub>2</sub>/MeOH 25:1); yellow amorphous powder (37%). <sup>1</sup>H NMR (400 MHz, [D<sub>6</sub>]DMSO): δ = 9.86 (br s, 2H, OH), 7.37 (d, *J*<sub>H,H</sub> = 8.8 Hz, 2H, CH=CH-C=O), 7.26 (d, *J*<sub>H,H</sub> = 7.2 Hz, 2H, Ar-H), 7.24 (d, *J*<sub>H,H</sub> = 6.8 Hz, 2H, Ar-H), 6.35 (d, *J*<sub>H,H</sub> = 10.0 Hz, 2H, CH=CH-C=O) ppm. <sup>13</sup>C NMR (100 MHz, [D<sub>6</sub>]DMSO): δ = 159.7 (C=O), 151.4 (Ar), 147.1 (CH=CH-C=O), 142.2 (Ar), 119.8 (Ar), 118.5 (Ar), 117.3 (Ar), 117.0 (Ar), 116.1 (CH=CH-C=O) ppm. MS (ESI): *m/z* calcd for C<sub>18</sub>H<sub>11</sub>O<sub>6</sub> = 323.05 [M+H]<sup>+</sup>; found: 323.06; HRMS (ESI): *m/z* calcd for C<sub>18</sub>H<sub>9</sub>O<sub>6</sub> = 321.0405 [M-H]<sup>-</sup>; found: 321.0408; elemental analysis calcd (%) for C<sub>18</sub>H<sub>10</sub>O<sub>6</sub>: C 67.09, H 3.13, O 29.79; found: C 67.13, H 3.17, O 29.82 (for the full characterization of compound **4g** see ref. [45]).

Bicoumarin **4g'**: *R*<sub>f</sub> = 0.23 (CH<sub>2</sub>Cl<sub>2</sub>/MeOH 25:1); yellow amorphous powder (40%). <sup>1</sup>H NMR (400 MHz, [D<sub>6</sub>]DMSO): δ = 10.01 (br s, 1H, OH), 7.99 (d, *J*<sub>H,H</sub> = 9.6 Hz, 1H, CH=CH-C=O), 7.88 (d, *J*<sub>H,H</sub> = 9.6 Hz, 1H, CH=CH-C=O), 7.40 (d, *J*<sub>H,H</sub> = 8.6 Hz, 1H, Ar-H), 7.26–7.22 (m, 3H, Ar-H), 7.10 (d, *J*<sub>H,H</sub> = 2.8 Hz, 1H, Ar-H), 6.48 (d, *J*<sub>H,H</sub> = 9.6 Hz, CH=CH-C=O), 6.44 (d, *J*<sub>H,H</sub> = 9.6 Hz, CH=CH-C=O) ppm. <sup>13</sup>C NMR (100 MHz, [D<sub>6</sub>]DMSO): δ = 159.8 (C=O), 159.5 (C=O), 154.1 (Ar), 148.6 (Ar), 146.7 (Ar), 145.9 (Ar), 143.6 (CH=CH-C=O), 137.9 (CH=CH-C=O), 135.9 (Ar), 121.0 (Ar), 119.7 (Ar), 119.2 (Ar), 117.5 (Ar), 116.77 (CH=CH-C=O), 116.73 (CH=CH-C=O), 114.0 (Ar), 113.7 (Ar), 112.5 (Ar) ppm. MS (ESI): *m/z* calcd for C<sub>18</sub>H<sub>11</sub>O<sub>6</sub> = 323.05 [M+H]<sup>+</sup>; found: 323.03; HRMS (ESI): *m/z* calcd for C<sub>18</sub>H<sub>9</sub>O<sub>6</sub> = 321.0405 [M-H]<sup>-</sup>; found: 321.0407; elemental analysis calcd (%) for C<sub>18</sub>H<sub>10</sub>O<sub>6</sub>: C 67.09, H 3.13, O 29.79; found: C 67.07, H 3.13, O 29.80 (for the full characterization of compound **4g'** see ref. [45]).

## Acknowledgements

We thank Dr. Massimo Zippilli and Franco Zippilli (Elettromeccanica Franco Zippilli snc.) for providing blue-LED apparatus, and Fondazione Toscana Life Sciences (TLS) for providing the High-Resolution Mass Spectrometric analyses. CGA (Centro Grandi Apparecchiature, University of Tuscia) and PRIN 2017 project "ORIGINALE CHEMIAE" in Antiviral Strategy – Origin and Modernization of Multi-Component Chemistry as a Source of Innovative Broad Spectrum Antiviral Strategy, cod.2017BMK8JR (L. B. and R. S.) are acknowledged. Open Access Funding provided by Università degli Studi della Tuscia within the CRUI-CARE Agreement.

## Conflict of Interest

The authors declare no conflict of interest.

**Keywords:** Photobiocatalysis • Blue-LED • Peroxidase • C–C coupling • Bicoumarin

- [1] J. N. Rodríguez-López, D. J. Lowe, J. Hernández-Ruiz, A. N. P. Hiner, F. García-Cánovas, R. N. F. Thorneley, *J. Am. Chem. Soc.* **2001**, *123*, 11838–11847.
- [2] C. M. Casadei, A. Gumiero, C. L. Metcalfe, E. J. Murphy, J. Basran, M. G. Concilio, S. C. M. Teixeira, T. E. Schrader, A. J. Fielding, A. Ostermann, M. P. Blakeley, E. L. Raven, P. C. E. Moody, *Science (80-)*. **2014**, *345*, 193–197.
- [3] S. G. Sligar, *Science (80-)*. **2010**, *330*, 924–925.
- [4] W. B. Geoghegan, in *Enzym. Immunoass.* (Eds.: T. T. Ngo, H. M. Lenhoff), Springer US, Boston, MA, **1985**, pp. 451–465.
- [5] A. Kobayashi, Y. Koguchi, H. Kanzaki, S. Kajiyama, K. Kawazu, *Biosci. Biotechnol. Biochem.* **1994**, *58*, 133–134.
- [6] F. Saliu, E.-L. Tolppa, L. Zoia, M. Orlandi, *Tetrahedron Lett.* **2011**, *52*, 3856–3860.
- [7] L. M. M. Mouterde, A. L. Flourat, M. M. M. Cagnet, P.-H. Ducrot, F. Allais, *Eur. J. Org. Chem.* **2013**, *2013*, 173–179.
- [8] M. B. Arnao, M. Acosta, J. A. del Rio, F. García-Cánovas, *Biochim. Biophys. Acta Protein Struct. Mol. Enzymol.* **1990**, *1038*, 85–89.
- [9] J. Hernández-Ruiz, M. B. Arnao, A. N. P. Hiner, F. García-Cánovas, M. Acosta, *Biochem. J.* **2001**, *354*, 107–114.
- [10] B. O. Burek, S. Bormann, F. Hollmann, J. Z. Bloh, D. Holtmann, *Green Chem.* **2019**, *21*, 3232–3249.
- [11] C. E. Grey, F. Rundbäck, P. Adlercreutz, *J. Biotechnol.* **2008**, *135*, 196–201.
- [12] M. P. J. Van Deurzen, I. J. Remkes, F. Van Rantwijk, R. A. Sheldon, *J. Mol. Catal. A* **1997**, *117*, 329–337.
- [13] M. P. J. Van Deurzen, K. Seelbach, F. van Rantwijk, U. Kragl, R. A. Sheldon, *Biocatal. Biotransformation* **1997**, *15*, 1–16.
- [14] A. E. V. Hagström, U. Törnvall, M. Nordblad, R. Hatti-Kaul, J. M. Woodley, *Biotechnol. Prog.* **2011**, *27*, 67–76.
- [15] S. B. Bankar, M. V. Bule, R. S. Singhal, L. Ananthanarayan, *Biotechnol. Adv.* **2009**, *27*, 489–501.
- [16] F. Tieves, S. J.-P. Willot, M. M. C. H. van Schie, M. C. R. Rauch, S. H. H. Younes, W. Zhang, J. Dong, P. de Santos, J. M. Robbins, B. Bommarius, M. Alcalde, A. S. Bommarius, F. Hollmann, *Angew. Chem. Int. Ed.* **2019**, *58*, 7873–7877; *Angew. Chem.* **2019**, *131*, 7955–7959.
- [17] H. L. Wapshott-Stehli, A. M. Grunden, *Enzyme Microb. Technol.* **2021**, *145*, 109744.
- [18] E. Churakova, M. Kluge, R. Ullrich, I. Arends, M. Hofrichter, F. Hollmann, *Angew. Chem. Int. Ed.* **2011**, *50*, 10716–10719; *Angew. Chem.* **2011**, *123*, 10904–10907.
- [19] D. I. Perez, M. M. Grau, I. W. C. E. Arends, F. Hollmann, *Chem. Commun.* **2009**, 6848–6850.
- [20] W. Zhang, B. O. Burek, E. Fernández-Fueyo, M. Alcalde, J. Z. Bloh, F. Hollmann, *Angew. Chem. Int. Ed.* **2017**, *56*, 15451–15455; *Angew. Chem.* **2017**, *129*, 15654–15658.
- [21] C. J. Seel, A. Králík, M. Hacker, A. Frank, B. König, T. Gulder, *ChemCatChem* **2018**, *10*, 3960–3963.
- [22] S. J.-P. Willot, E. Fernández-Fueyo, F. Tieves, M. Pesic, M. Alcalde, I. W. C. E. Arends, C. B. Park, F. Hollmann, *ACS Catal.* **2019**, *9*, 890–894.
- [23] T. Krieg, S. Hüttmann, K.-M. Mangold, J. Schrader, D. Holtmann, *Green Chem.* **2011**, *13*, 2686–2689.
- [24] S. Bormann, M. M. C. H. van Schie, T. P. De Almeida, W. Zhang, M. Stöckl, R. Ulber, F. Hollmann, D. Holtmann, *ChemSusChem* **2019**, *12*, 4759–4763.
- [25] F. Harnisch, D. Holtmann, *Bioelectrosynthesis*, Springer, **2019**.
- [26] K. Ryu, J. S. Dordick, *Biochemistry* **1992**, *31*, 2588–2598.
- [27] E. Churakova, I. W. C. E. Arends, F. Hollmann, *ChemCatChem* **2013**, *5*, 565–568.
- [28] M. C. R. Rauch, F. Tieves, C. E. Paul, I. W. C. E. Arends, M. Alcalde, F. Hollmann, *ChemCatChem* **2019**, *11*, 4519–4523.
- [29] M. Hobisch, M. M. C. H. van Schie, J. Kim, K. Røjkjær Andersen, M. Alcalde, R. Kourist, C. B. Park, F. Hollmann, S. Kara, *ChemCatChem* **2020**, *12*, 4009–4013.
- [30] J. M. Woodley, M. D. Lilly, in *Biocatal. Non-Conventional Media* (Eds.: J. Tramper, M. H. Vermüe, H. H. Beftink, U. B. T.-P. in B. von Stockar), Elsevier, **1992**, pp. 147–154.
- [31] I. P. Rosinha Grundtvig, S. Heintz, U. Krühne, K. V. Gernaey, P. Adlercreutz, J. D. Hayler, A. S. Wells, J. M. Woodley, *Biotechnol. Adv.* **2018**, *36*, 1801–1814.
- [32] C. Zippilli, L. Botta, B. M. Bizzarri, M. C. Baratto, R. Pogni, R. Saladino, *RSC Adv.* **2020**, *10*, 10897–10903.
- [33] C. Zippilli, L. Botta, B. M. Bizzarri, L. Nencioni, M. De Angelis, V. Protto, G. Giorgi, M. C. Baratto, R. Pogni, R. Saladino, *Int. J. Mol. Sci.* **2021**, *22*, DOI 10.3390/ijms22031337.
- [34] S. Monticelli, L. Castoldi, I. Murgia, R. Senatore, E. Mazzeo, J. Wackerlig, E. Urban, T. Langer, V. Pace, *Monatsh. Chem.* **2017**, *148*, 37–48.

- [35] A. Ismael, A. Gevorgyan, T. Skrydstrup, A. Bayer, *Org. Process Res. Dev.* **2020**, *24*, 2665–2675.
- [36] A. Sagadevan, K. C. Hwang, M.-D. Su, *Nat. Commun.* **2017**, *8*, 1812.
- [37] S. Zakavi, H. Yavari, A. Heydari-turkmani, L. Alghooneh, *J. Catal.* **2020**, *387*, 84–94.
- [38] J.-H. Shon, D. Kim, M. D. Rathnayake, S. Sittel, J. Weaver, T. S. Teets, *Chem. Sci.* **2021**, *12*, 4069–4078.
- [39] R. Nasrollahi, A. Heydari-turkmani, S. Zakavi, *Catal. Sci. Technol.* **2019**, *9*, 1260–1272.
- [40] R. Ravanfar, A. Abbaspourrad, *Green Chem.* **2020**, *22*, 6105–6114.
- [41] Z.-Y. Yang, J.-T. Kan, Z.-Y. Cheng, X.-L. Wang, Y.-Z. Zhu, W. Guo, *Cytotechnology* **2014**, *66*, 51–61.
- [42] P. Zhou, Y. Takaishi, H. Duan, B. Chen, G. Honda, M. Itoh, Y. Takeda, O. K. Kodzhimatov, K.-H. Lee, *Phytochemistry* **2000**, *53*, 689–697.
- [43] B. M. Bizzarri, L. Botta, E. Capecchi, I. Celestino, P. Checconi, A. T. Palamara, L. Nencioni, R. Saladino, *J. Nat. Prod.* **2017**, *80*, 3247–3254.
- [44] R. Pratap, V. J. Ram, *Chem. Rev.* **2014**, *114*, 10476–10526.
- [45] X. Gao, S. Huang, P. Dong, C. Wang, J. Hou, X. Huo, B. Zhang, T. Ma, X. Ma, *Catal. Sci. Technol.* **2016**, *6*, 3585–3593.
- [46] M. Baune, K. Kang, W. D. C. Schenkeveld, S. M. Kraemer, H. Hayen, G. Weber, *BioMetals* **2020**, *33*, 305–321.
- [47] P. Castaldi, G. Garau, A. Palma, S. Deiana, *J. Inorg. Biochem.* **2012**, *108*, 30–35.
- [48] T. A. Enache, A. M. Oliveira-Brett, *J. Electroanal. Chem.* **2011**, *655*, 9–16.
- [49] W. E. Blumberg, J. Peisach, B. A. Wittenberg, J. B. Wittenberg, *J. Biol. Chem.* **1968**, *243*, 1854–1862.
- [50] I. G. Gazaryan, L. M. Lagrimini, *Phytochemistry* **1996**, *41*, 1029–1034.
- [51] R. L. Osborne, M. K. Coggins, G. M. Raner, M. Walla, J. H. Dawson, *Biochemistry* **2009**, *48*, 4231–4238.
- [52] J. H. Dawson, M. Sono, *Chem. Rev.* **1987**, *87*, 1255–1276.
- [53] J. Zhang, Y. Nosaka, *J. Phys. Chem. C* **2013**, *117*, 1383–1391.
- [54] A. C. Maier, E. H. Iglebaek, M. Jonsson, *ChemCatChem* **2019**, *11*, 5435–5438.
- [55] V. Leandri, J. M. Gardner, M. Jonsson, *J. Phys. Chem. C* **2019**, *123*, 6667–6674.
- [56] J. Liu, Z. Feng, J. Xu, Y. Wang, P. Zhang, *Phytochemistry* **2007**, *68*, 1775–1780.
- [57] L. Fan, Y. Wang, N. Liang, X.-J. Huang, M.-M. Li, C.-L. Fan, Z.-L. Wu, Y.-L. Li, W.-C. Ye, *Planta Med.* **2013**, *79*, 1558–1564.
- [58] L. Dai, A. M. Klivanov, *Proc. Nat. Acad. Sci.* **1999**, *96*, 9475–9478.
- [59] S.-F. Wang, T. Chen, Z.-L. Zhang, D.-W. Pang, *Electrochem. Commun.* **2007**, *9*, 1337–1342.
- [60] H. U. Bergmeyer, K. Gawehn, *Methods of Enzymatic Analysis*, Academic Press, **1974**.

---

Manuscript received: May 24, 2021

Revised manuscript received: July 26, 2021

Accepted manuscript online: July 27, 2021

Version of record online: August 12, 2021